Int. J. Advanced Design and Manufacturing Technology, 2023, Vol. 16, No. 2, pp. 35-43

DOI: 10.30486/admt.2022.697460 ISSN: 2252-0406 https://admt.isfahan.iau.ir

Vibration Behavior of the Planetary Gear System by Considering the Fixed Output

Ali Shahabi[1]
Department of Mechanical Engineering,
University of Sistan and Baluchestan, Zahedan, Iran
Nedayedanesh Institute of Higher Education of Hormozgan, Bandar Abbas, Iran
E-mail: alishahabi@pgs.usb.ac.ir

Amir Hossein Kazemian[2, *]
Department of Mechanical Engineering,
University of Sistan and Baluchestan, Zahedan, Iran
E-mail: kazemian@eng.usb.ac.ir
*Corresponding author

Received: 8 April 2022, Revised: 7 August 2022, Accepted: 7 August 2022

Abstract: This work studies on analytical model of the single–stage spur planetary gear in form of lumped–parameter model. It includes key nonlinear factors of planetary gear vibration such as mesh stiffness and backlash of meshing gears. The planetary gear set is modeled as a set of lumped masses and springs and dynamic model of the planetary gear set is presented. Nonlinear equations of motion are presented for each component and each component has three degrees of freedom in planar motion. We have numerically evaluated a set of linear and nonlinear equations to obtain natural frequencies and analysis of vibration behavior of the system under nonlinear factors and fixed output. In previous researches, natural frequencies of planetary gears were evaluated from two points of view: the first one considered fixed output for planetary gears and the second one consists of free rotational output. In this research, the influence of the output flexibility is evaluated on natural frequencies of the planetary gear. Meanwhile, by considering the fixed output, vibration behavior of the nonlinear system is investigated. Results show that the most important effect of the output flexibility is on the principal natural frequency. Because of chaotic phenomenon, vibration behavior of components in translational directions is different.

Keywords: Backlash, Chaotic Phenomenon, Mesh Stiffness, Natural Frequency, Spur Planetary Gear

Biographical notes: Ali Shahabi is a PhD student in Mechanical Engineering at University of Sistan and Baluchestan, Zahedan, Iran. He is currently lecturer at Nedayedanesh Institute of Higher Education of Hormozgan, Bandar Abbas, Iran. He received his MSc in Mechanical Engineering from Shahid Bahonar University of Kerman in 2014. **Amir Hossein Kazemian** received his PhD in Mechanical Engineering from Shahid Bahonar University of Kerman in 2017. He is currently Assistant Professor of Mechanical engineering at University of Sistan and Baluchestan, Zahedan, Iran. His current research focuses on dynamic, vibration and control of suspension and vehicle systems.

Research paper

1 INTRODUCTION

The single–stage spur planetary gear set consists of carrier, ring, sun and planets. In order to vibration behavior analysis of the planetary gear system, time–varying mesh stiffness, backlash of sun–planets and ring–planets and output flexibility are important factors. Lin and Parker [1] modelled the time–varying mesh stiffness of the sun–planet and ring–planet meshes as rectangular waveforms with different contact ratios and mesh phasing. In order to study on a dynamic model of the gear pair with multi-state mesh and time-varying parameters, Shi et al. [2] considered effects of teeth separation and back–side tooth mesh. Sun and Ha [3] presented the nonlinear dynamics of a planetary gear system with time–varying mesh stiffness, backlash and error excitation. Several researchers studied on planetary gear natural frequencies and vibration modes. Kahraman [4-5] studied on planetary gear models to evaluate natural frequencies and vibration modes and also, he predicted that a dynamic load sharing factor can be used in the dynamic model. Ambarisha and Parker [6] showed that planet modes are one of three categories of planetary gear vibration modes and the symmetry of planetary gear systems and gear tooth mesh periodicity are sufficient to establish rules to suppress planet modes. Lin and Parker [7–9] studied analytically on modal properties of planetary gears to evaluate natural frequencies and vibration modes. Parker and Lin [10] also showed that the multiple tooth meshes in planetary gears have varying numbers of teeth in contact under operating speed, and these numbers of teeth all fluctuate at the same mesh frequency. Tatar et al. [11] created the dynamic model by using a lumped parameter model of the planetary gearbox and they assumed gears and carrier in the planetary gearbox are rigid. Nonlinear dynamic behavior of gears was examined using two models [12-13]: lumped–parameter model and finite element model. Li et al. [14] established a batch module called ‘‘integration of finite element analysis and optimum design’’ by taking gear systems as testing examples. Meanwhile, a dynamic lumped–parameter gear model incorporating the effects of time–varying and asymmetric mesh stiffness nonlinearity, was formulated by Chen et al. [15] to analyze the spur gear rattle response under the idling condition. A nonlinear time–varying dynamic model for a planetary gear system and new analytical formula of tooth deflections have been investigated in [16-17]. Moreover, for some structures of planetary gear, gear systems and other dynamical systems, vibration characteristics [18-19], dynamic analysis [20–24] and modal properties [25] have been investigated.

This research presents the linear and nonlinear dynamic modelling of the planetary system to study on natural frequencies and vibration behaviour of the system. The system is considered as rotational system and in rotational planetary system, the degrees of freedom of components in translational directions are negligible and components of the system have freedom only in rotational direction. The sun gear and carrier are considered as input and output powers and the ring gear is held stationary. Fixed or floating of the sun, ring and carrier bearings are simulated by bearing stiffness. As an example, free rotation of the carrier is modeled by zero carrier rotational stiffness and severe resistance of the output against the rotation is modeled by huge carrier rotational stiffness. For the linear system, the effect of the output rigidity/flexibility on natural frequencies is studied. To study the effect of the output rigidity on natural frequencies, fixed or floating of the output by using its rotational stiffness is simulated to show the output rigidity or flexibility. The sun gear as an input is considered fixed or floating and for both cases of fixed sun and floating sun (the input power), natural frequencies are defined as function of the carrier (the output power) rotational flexibility. In order to study on planetary gear vibration, study on main sources of vibration; i.e., the mesh stiffness and backlash of meshing gears is necessary. Nonlinear equations of motion are solved by numerical integration method with RADAU5 algorithm (implicit Runge–Kutta method of order 5 (Radau IIA), [26–28]) to study on vibration behaviour of the system by considering time–varying mesh stiffness, backlash of meshing gears and fixed output.

2 MODELING OF THE PLANETARY GEAR DYNAMIC

Fig. 1 shows two–dimensional (2D) lumped–parameter model of the planetary gear system.

Each element such as carrier (c), ring (r), sun (s), J planets is assumed to have rigid behavior, i.e., lumped parameter system. Sun and carrier are connected to the input and output shaft respectively; the external torque is applied to the input shaft (τ_s) and the ring gear is held stationary. Mass and moment of inertia of bearings are: m_i and I_i for $i = c, r, s, j$ and $j = 1, 2, \dots, J$. The base radius for bearings of the carrier, ring, sun and planets is shown by $r_i, i = c, r, s, j$. For the carrier bearing r is the radius of the circle passing through the center of planets. For translational stiffness of bearings ($K_{ix}, K_{iy}, i = c, r, s$), bearings are modeled by springs in x and y directions. Rotational stiffness of bearings ($K_{iu}, i = c, r, s$) is modeled by springs in rotational direction of u where $u_i = r_i\theta_i,\ i = c, r, s$ and θ is the rotation of components. Stiffness for planet bearings is shown by K_j and translational and rotational coordinates of the carrier, ring and sun are: x_i, y_i and u_i

where $i = c, r, s$. The radial and tangential coordinates are: ξ_j and η_j (translational coordinates of the planet center) and rotational coordinate of planets is: $u_j = r_j\theta_j$ and θ_j is the rotation of planets. The circumferential j[th] planet location is identified by time–varying angle of $\Omega_j(t)$. The circumferential j[th] planet location depends on the unit vector's rotation (**i**-unit vector) and measure counter–clockwise from the first planet, so that $\Omega_1 = 0$. Each element has three degrees of freedom in planar motion: two translations and one rotation, so the system has $3(J + 3)$ degrees of freedom where J is number of planets.

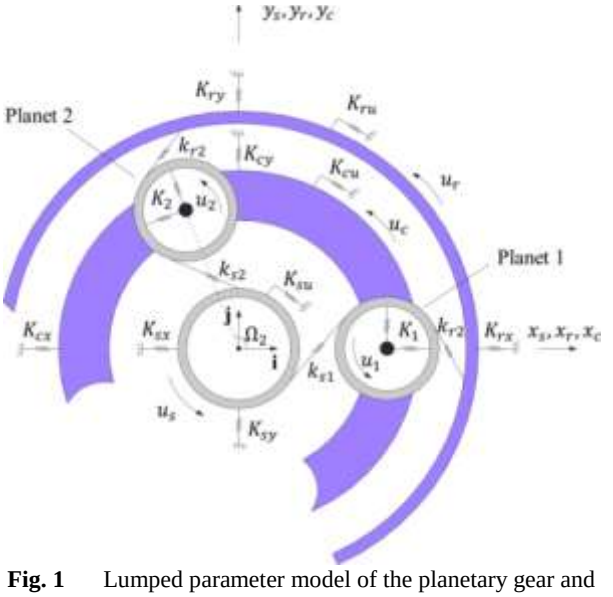

Fig. 1 Lumped parameter model of the planetary gear and system coordinates.

2.1. Equations of Motion

Ring– j[th] planet and sun– j[th] planet meshes are shown in "Fig. 2". As an example, in "Fig. 2", mesh stiffness between ring and j[th] planet ($k_{rj}(t)$) acting along the line of action.

Static transmission error of the ring– j[th] planet ($e_{rj}(t)$) is included as dynamic excitation at the mesh spring. In the present model, flexibilities of the gear teeth and gear bodies are simulated by springs (reciprocal actions of gear mesh modeled as springs). Variation of tooth contact conditions results the periodically time–varying stiffness of meshing gears along the line of action. Springs elements have a clearance that represents the backlash of meshing gears by $2b_r$ and $2b_s$.

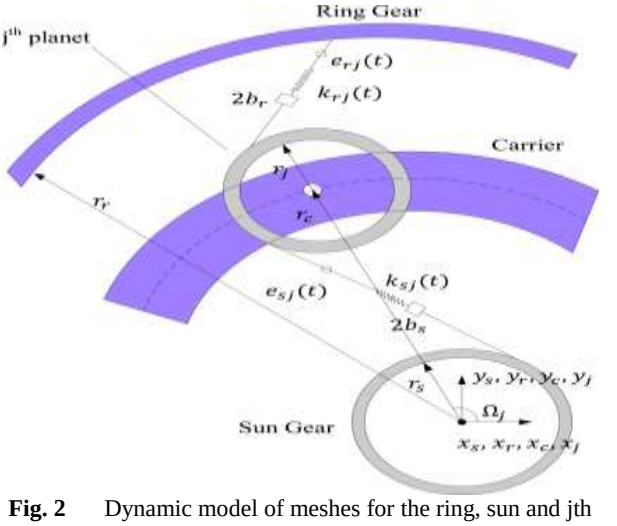

Fig. 2 Dynamic model of meshes for the ring, sun and jth planet.

$k_{rj}(t)$ and $k_{sj}(t)$ are mesh stiffness of the ring– j[th] planet and sun– j[th] planet. By using the model of "Fig. 3", the mesh stiffness of meshing gears is considered [1].

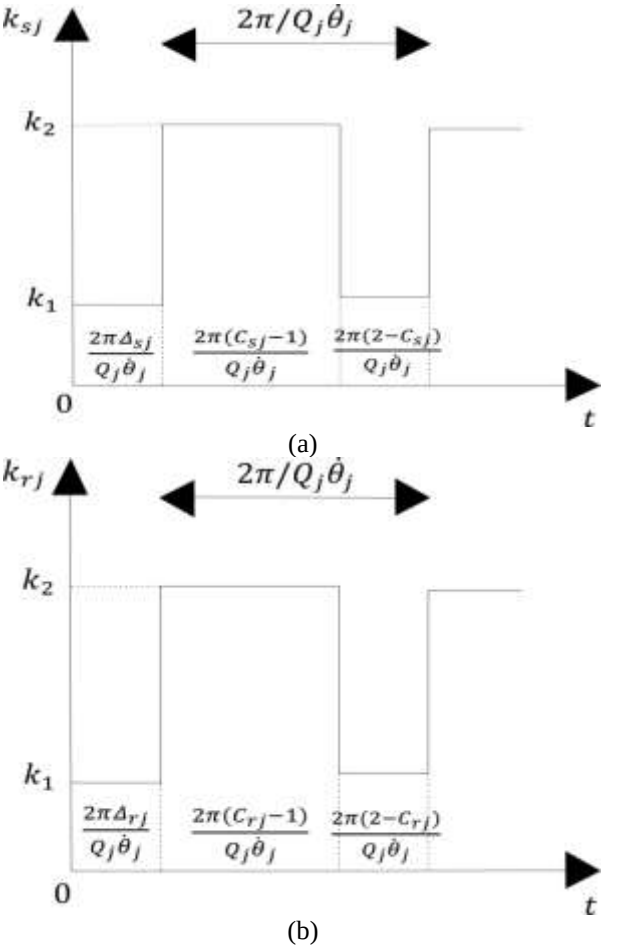

Fig. 3 Mesh stiffness model of the: (a) sun– j[th] planet and (b) ring– j[th] planet.

In "Fig. 3", the stiffness of one and two pair of teeth is available (k_1 and k_2, respectively) and for meshing gears the mesh phasing is $\Delta_{sj}= \Omega_j Q_s/2\pi$ and $\Delta_{rj}= \Omega_j Q_r/2\pi$ where Q is the tooth number of gears. By considering contact ratio between the sun– j[th] planet and the ring– j[th] as C_{sj} and C_{rj}, the mesh stiffness of them is obtained as "Eq. (1)".

$$k_{sj}(t)=\begin{Bmatrix} k_2 \quad if \quad \dfrac{2\pi(l-1)}{Q_j\dot{\theta}_j}<t<\dfrac{2\pi(C_{sj}+l-2)}{Q_j\dot{\theta}_j} \\ k_1 \quad if \quad \dfrac{2\pi(C_{sj}+l-2)}{Q_j\dot{\theta}_j}<t<\dfrac{2\pi l}{Q_j\dot{\theta}_j} \end{Bmatrix}$$

,

$$k_{rj}(t)=\begin{Bmatrix} k_2 \quad if \quad \dfrac{2\pi(l-1)}{Q_j\dot{\theta}_j}<t<\dfrac{2\pi(C_{rj}+l-2)}{Q_j\dot{\theta}_j} \\ k_1 \quad if \quad \dfrac{2\pi(C_{rj}+l-2)}{Q_j\dot{\theta}_j}<t<\dfrac{2\pi l}{Q_j\dot{\theta}_j} \end{Bmatrix} \quad (1)$$

Where, l is an integer. Note that, because of mesh phasing relationships [10], mesh stiffness of the sun– j[th] planet ($j = 2,3,...$) is function of: 1. mesh stiffness of the sun–first planet and 2. relative phase between the sun– j[th] planet ($j = 2,3,...$) and the sun–first planet. This is similar for mesh stiffness of the ring– j[th] planet ($j = 2,3,...$). In this study all the sun– j[th] planet and the ring– j[th] planet meshes are in phase with each other.

The basic dynamical equilibrium equations contain $3(J+3)$ nonlinear ordinary differential equations. By using Newton's second law, equations of motion for the ring gear in x, y and u directions are obtained as "Eqs. (2-4)":

$$m_r\ddot{x}_r-\sum_{j=1}^{J}[k_{rj}(t).B_{rx}.\delta_{rj}.\sin(\Omega_j+\alpha_{rj})]+K_{rx}x_r=0 \quad (2)$$

$$m_r\ddot{y}_r+\sum_{j=1}^{J}[k_{rj}(t).B_{ry}.\delta_{rj}.\cos(\Omega_j+\alpha_{rj})]+K_{ry}y_r=0 \quad (3)$$

$$\frac{I_r}{r_r^{\,2}}\ddot{u}_r+\sum_{j=1}^{J}\left[k_{rj}(t).B_{ru}.\delta_{rj}\right]+K_{ru}u_r=0 \quad (4)$$

In "Eqs. (2-4)", x and y are the translational and u is the rotational degrees of freedom of the system. $\alpha_{rj}(t)$ is the pressure angle of the ring– j[th] planet and the backlash is modeled as function of B_r under the tolerance with domain of $2b_r$ (see, "Fig. 2"). Moreover, B_{rx}, B_{ry} and B_{ru} are the piecewise–linear movement functions for mesh of the ring– j[th] planet, and they are defined as "Eq. (5)" [16]:

$$B_{rx}=\begin{Bmatrix} x_r-x_j+\dfrac{b_r}{\sin(\Omega_j+\alpha_{rj})},\Gamma_r\geq b_r \\ 0,|\Gamma_r|<b_r \\ x_r-x_j-\dfrac{b_r}{\sin(\Omega_j+\alpha_{rj})},\Gamma_r\leq -b_r \end{Bmatrix}$$

$$B_{ry}=\begin{Bmatrix} y_r-y_j-\dfrac{b_r}{\cos(\Omega_j+\alpha_{rj})},\Gamma_r\geq b_r \\ 0,|\Gamma_r|<b_r \\ y_r-y_j+\dfrac{b_r}{\cos(\Omega_j+\alpha_{rj})},\Gamma_r\leq -b_r \end{Bmatrix} \quad (5)$$

$$B_{ru}=\begin{Bmatrix} u_r-u_j-b_r,\Gamma_r\geq b_r \\ 0,|\Gamma_r|<b_r \\ u_r-u_j+b_r,\Gamma_r\leq -b_r \end{Bmatrix}$$

$$\Gamma_r=[-(x_r-x_j)\sin(\Omega_j+\alpha_{rj})+(y_r-y_j)\cos(\Omega_j+\alpha_{rj})+(u_r-u_j)]$$

Similarly, equations of motion for the sun gear, carrier and j[th] planet in x, y and u directions are obtained as "Eqs. (6-19)":

2.1.2. Sun gear Equations

$$m_s\ddot{x}_s-\sum_{j=1}^{J}[k_{sj}(t).B_{sx}.\delta_{sj}.\sin(\Omega_j-\alpha_{sj})]+K_{sx}x_s=0 \quad (6)$$

$$m_s\ddot{y}_s+\sum_{j=1}^{J}[k_{sj}(t).B_{sy}.\delta_{sj}.\cos(\Omega_j-\alpha_{sj})]+K_{sy}y_s=0 \quad (7)$$

$$\frac{I_s}{r_s^{\,2}}\ddot{u}_s+\sum_{j=1}^{J}\left[k_{sj}(t).B_{su}.\delta_{sj}\right]+K_{su}u_s=\frac{\tau_s}{r_s} \quad (8)$$

In "Eq. (8)", τ_s is the input torque applied on sun gear and:

$$B_{sx}=\begin{Bmatrix} x_j-x_s-\dfrac{b_s}{\sin(\Omega_j-\alpha_{sj})},\Gamma_s\geq b_s \\ 0,|\Gamma_s|<b_s \\ x_j-x_s+\dfrac{b_s}{\sin(\Omega_j-\alpha_{sj})},\Gamma_s\leq -b_s \end{Bmatrix}$$

$$B_{sy}=\begin{Bmatrix} y_j-y_s+\dfrac{b_s}{\cos(\Omega_j-\alpha_{sj})},\Gamma_s\geq b_s \\ 0,|\Gamma_s|<b_s \\ y_j-y_s-\dfrac{b_s}{\cos(\Omega_j-\alpha_{sj})},\Gamma_s\leq -b_s \end{Bmatrix} \quad (9)$$

$$B_{su} = \begin{cases} u_s + u_j - b_s, \Gamma_s \geq b_s \\ 0, |\Gamma_s| < b_s \\ u_s + u_j + b_s, \Gamma_s \leq -b_s \end{cases}$$

$$\Gamma_s = [(x_j - x_s)\sin(\Omega_j - \alpha_{sj}) - (y_j - y_s)\cos(\Omega_j - \alpha_{sj}) + (u_s + u_j)]$$

2.1.3. Carrier Equations

$$m_c \ddot{x}_c + \sum_{j=1}^{J} K_j.[\delta_{jr}.\cos\Omega_j - \delta_{jt}.\sin\Omega_j] + K_{cx} x_c = 0 \quad (10)$$

$$m_c \ddot{y}_c + \sum_{j=1}^{J} K_j.[\delta_{jr}.\sin\Omega_j + \delta_{jt}.\cos\Omega_j] + K_{cy} y_c = 0 \quad (11)$$

$$\frac{I_c}{r_c^2}\ddot{u}_c + \sum_{j=1}^{J} K_j.\delta_{jt} + K_{cu} u_c = 0 \quad (12)$$

2.1.4. jth Planet Equations

$$m_j \ddot{\xi}_j - k_{sj}(t).\delta_{sj}.\sin\alpha_{sj} + k_{rj}(t).\delta_{rj}.\sin\alpha_{rj} - K_j \delta_{jr} = 0 \quad (13)$$

$$m_j \ddot{\eta}_j - k_{sj}(t).\delta_{sj}.\cos\alpha_{sj} - k_{rj}(t).\delta_{rj}.\cos\alpha_{rj} - K_j \delta_{jt} = 0 \quad (14)$$

$$\frac{I_j}{r_j^2}\ddot{u}_j + k_{sj}(t).\delta_{sj} - k_{rj}(t).\delta_{rj} = 0 \quad (15)$$

In "Eqs. (2-15)", δ is compressions of the elastic elements (springs) and defined as "Eqs. (16-19)":

2.1.5. Sun– jth Planet Bearings Mesh

$$\delta_{sj} = \cos(\Omega_j - \alpha_{sj}).y_s - \sin(\Omega_j - \alpha_{sj}).x_s - \sin\alpha_{sj}.\xi_j - \cos\alpha_{sj}.\eta_j + u_s + u_j + e_{sj}(t) \quad (16)$$

2.1.6. Ring– jth Planet Bearings Mesh

$$\delta_{rj} = \cos(\Omega_j + \alpha_{rj}).y_r - \sin(\Omega_j + \alpha_{rj}).x_r + \sin\alpha_{rj}.\xi_j - \cos\alpha_{rj}.\eta_j + u_r - u_j + e_{rj}(t) \quad (17)$$

2.1.7 jth Planet Bearing Radial

$$\delta_{jr} = \sin\Omega_j.y_c + \cos\Omega_j.x_c - \xi_j \quad (18)$$

2.1.8 jth Planet Bearing Tangential

$$\delta_{jt} = \cos\Omega_j.y_c - \sin\Omega_j.x_c - \eta_j + u_c \quad (19)$$

Equations of motion for the system in the matrix form can be written as "Eq. (20)":

$$\mathbf{M}\ddot{\mathbf{q}}(t) + \left[\mathbf{K_m}(t) + \mathbf{K_b}\right]\mathbf{q}(t) = \boldsymbol{\tau}(t) \quad (20)$$

Where, $\mathbf{M}$ is the inertia matrix, $\mathbf{K}_b$ is the diagonal support stiffness matrix, $\mathbf{K}_m(t)$ is the symmetric stiffness matrix from coupling between components and $\boldsymbol{\tau}(t)$ is the external torque applied on the sun gear. Vector of general coordinates of the system is considered as "Eq. (21)":

$$\mathbf{q} = [x_c, y_c, u_c, x_r, y_r, u_r, x_s, y_s, u_s, \xi_j, \eta_j, u_j, ..., \xi_J, \eta_J, u_J]^{\mathrm{T}} \quad (21)$$

In order to evaluate natural frequencies, the associated eigenvalue problem of "Eq. (21)" is obtained as "Eq. (22)":

$$[-\omega_i^2\mathbf{M} + (\mathbf{K}_b + \mathbf{K}_m(t))]\boldsymbol{\varphi}_i = \mathbf{0} \quad (22)$$

Where, $\omega_i, , i = 1, \ldots, 3(3 + J)$ are natural frequencies and $\boldsymbol{\varphi}_i$ are vector of vibration modes. Vibration modes are classified into three types of translational, rotational and planet modes [7].

3 NUMERICAL RESULTS

To evaluate natural frequencies of the rotational system, parameters of "Table 1" and $k_1 = 3 \times 10^8$N/m and $k_2 = 7 \times 10^8$N/m are considered.

Table 1 Numerical parameters of the planetary gear set

	Carrier	Ring	Sun	Planet
I/r^2 (kg)	6.29	3	0.39	0.61
Mass (kg)	5.43	2.35	0.4	0.66
Base dia. (mm)	176.8	275	77.4	100.3
Translational stiffnesses (N/m)	10^8	10^8	10^8	10^8
Rotational stiffness (N/m)	0	10^9	0	—
Number of teeth	—	100	28	36
Torque (N.m)	—	—	1100	—
	Sun – j^{th} planet		Ring – j^{th} planet	
Pressure angle (degree)	24.6		24.6	
Contact ratio	1.48		1.642	

Validation of natural frequencies ($\omega_i, i = 1, \ldots, [3(J + 3)]$) with three equally spaced planets ($\Omega_j = 2\pi(j-1)/J: \Omega_1 = 0, \Omega_2 = 120, \Omega_3 = 240$ degrees, 18 degrees of freedom) are tabulated in "Table 2" by considering $K_{sx}, K_{sy} = 1 \times 10^8$ N/m as like as Ref. [7]. By considering output rotation (floating carrier), "Table 2" presents natural frequencies of the rotational system.

Table 2 Natural frequencies of the rotational system for this study and Ref. [7]

	Natural frequency (Hz)	Vibration mode
Three equally spaced planets and rotational system of this study	$\omega_1 = 0$	Rotational
	$\omega_2, \omega_3 = 743.5$ $\omega_4, \omega_5 = 1102.9$	Translational Translational
Three equally spaced planets and rotational system of Ref. [7]	$\omega_1 = 0$	Rotational
	$\omega_2, \omega_3 = 743.2$ $\omega_4, \omega_5 = 1102.4$	Translational Translational

For rotational systems, when K_{cu} is almost zero it means that the carrier (system output) is free to rotate and rigid body motion appears, see Ref. [7]. Moreover, large K_{cu} represents almost fixed output for the planetary gear system, so for this manner none of natural frequencies of the system are not zero and rigid body motion does not appear. When output of the system is fixed, the system is locked and vibration will be occurred. Meanwhile, small K_s represents floating sun and large K_s leads to fixed sun gear. Because of input rotation, the bearing rotational stiffness of the sun gear (K_{su}) for fixed and floating sun gear leads to the zero and ring gear is held stationary. Fig. 4 shows typical vibration modes for the rotational system with three equally spaced planets.

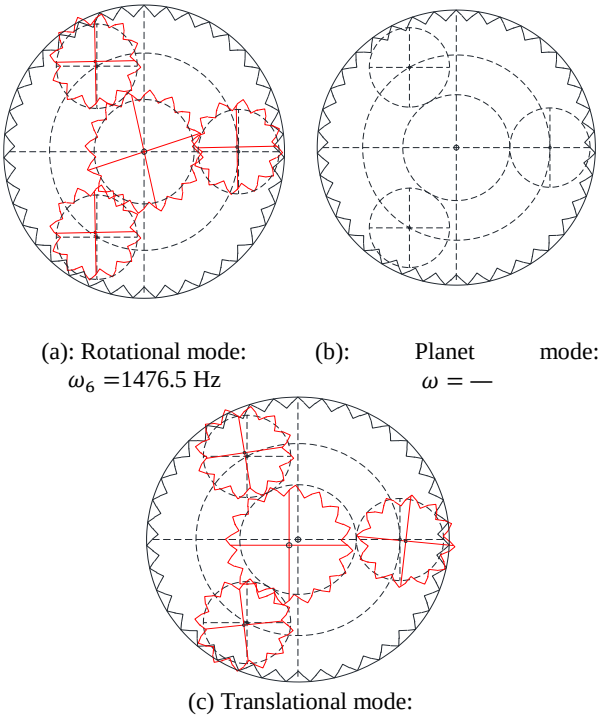

(a): Rotational mode: ω_6 =1476.5 Hz (b): Planet mode: ω = —

(c) Translational mode: $\omega_2 = 743.5$ Hz

Fig. 4 Types of vibration modes of the system with three equally spaced planets (0, 120 and 240 degrees).

Equilibrium and deflected positions are shown by dashed and solid lines. Note that, planet mode is appeared on the system, when numbers of planets are four or more than four [7].

For the rotational system, the sensitivity of first four natural frequencies to the output flexibility; i.e., carrier rotational stiffness (K_{cu}) with parameters of "Table 1", is shown in "Figs. 5 and 6" for both cases of fixed and floating sun gear.

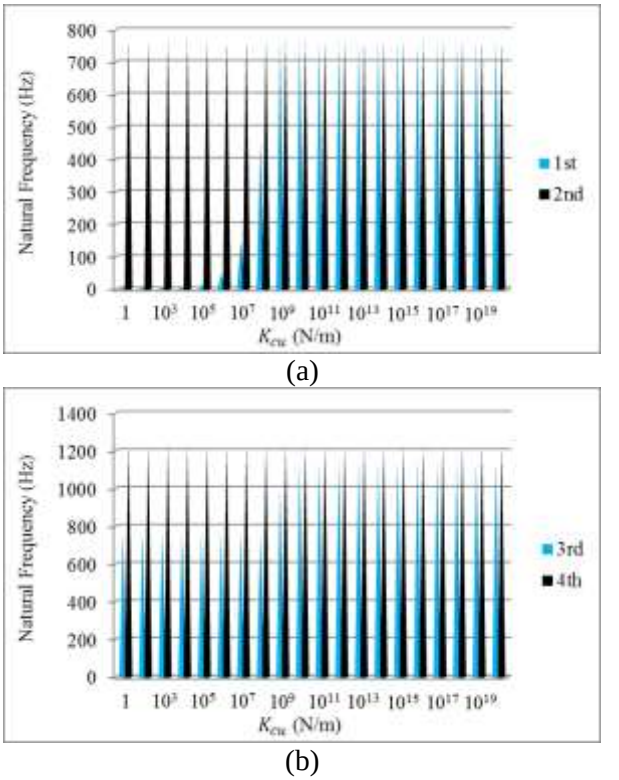

Fig. 5 The effect of the output flexibility on first four natural frequencies for the planetary gear system with fixed sun gear.

Fig. 5(a) for the case of fixed sun ($K_{sx}, K_{sy} \to \infty$), shows that for small values of K_{cu}, less than 10^5 N/m, the first natural frequency is almost zero; i.e., the system is semi–definite and rigid body motion appears. For large values of K_{cu}, more than 10^9 N/m, the first natural frequency remains constant at 766 Hz. By variation of the output flexibility (K_{cu}), the second natural frequency remains constant at 766 Hz. In "Fig. 5(b)", the third natural frequency increases from 766 Hz to 1150 Hz and varies about 50% and the forth natural frequency remains constant at 1226 Hz. In "Fig. 6(a)", for the case of floating sun gear ($K_{sx}, K_{sy} \to 0$), for small values of K_{cu} (less than 10^5 N/m), the first natural frequency is almost zero, so the system is semi–definite and the rigid body motion appears. When K_{cu} increases from 10^9 N/m to 10^{20} N/m, the first natural frequency varies more than 99% and remains unchangeable at 478Hz. Besides, the second natural frequency remains constant at 478 Hz. In "Fig. 6(b)",

the third natural frequency increases from 478 Hz to 850 Hz; i.e., varies about 77% and the forth natural frequency remains unchangeable at 850 Hz.

For both cases of fixed sun gear and floating sun gear, the output flexibility has a sensible effect on the first natural frequency. When rotational stiffness of the carrier is zero, the system possesses rigid body motion and the first natural frequency is zero.

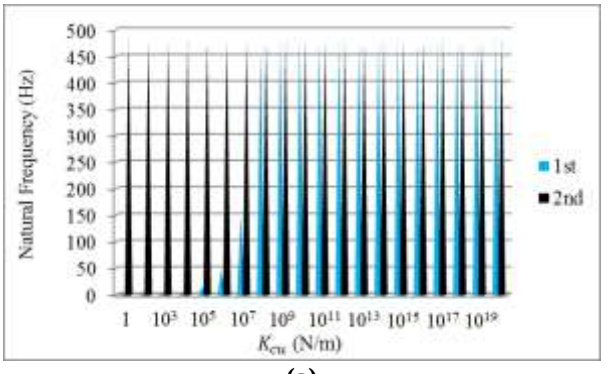

(a)

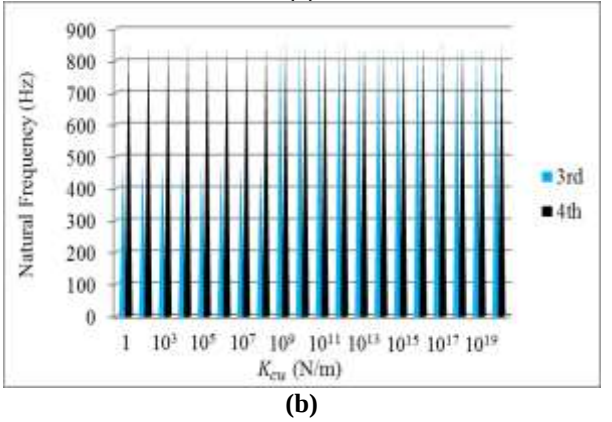

(b)

Fig. 6 The effect of the output flexibility at first for natural frequencies for the planetary gear system with floating sun gear.

For the nonlinear rotational system with fixed output, the mesh stiffness and backlash of meshing gears ($b_s = b_r = 1.5\,mm$) are considered. By using numerical integration method with RADAU5 algorithm (implicit Runge-Kutta method of order 5 (Radau IIA) [26-28], vibration behavior of the sun gear and first planet is obtained by numerical integration method and parameters of "Table 1" and shown in "Figs. 7 and 8". Study on the bifurcation phenomenon is one of the appropriate strategies to examine the instability in dynamical systems. Figure 7 shows that bifurcation diagrams of sun gear in x and y directions are different because of chaotic phenomenon. Meanwhile, Poincaré maps of sun gear are displayed in "Fig. 8". According to results, at range of 2500 Hz, the oscillation is occurred with double frequency of the excitation. Jump phenomenon is occurred nearly at frequency of 1300 Hz. Chaotic is available on the system up to frequency of 3000 Hz.

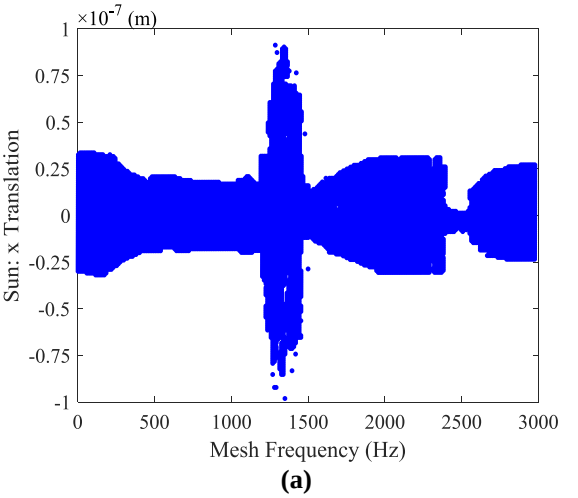

(a)

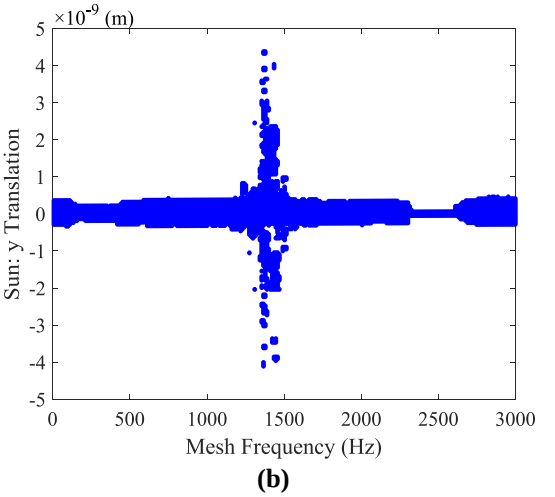

(b)

Fig. 7 Bifurcation diagrams of: (a): sun center x translation and, (b): sun center y translation.

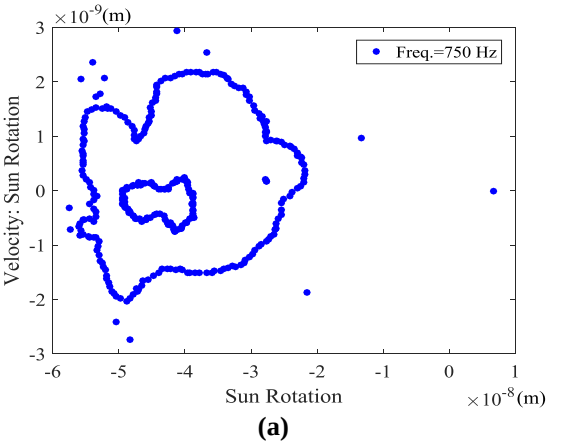

(a)

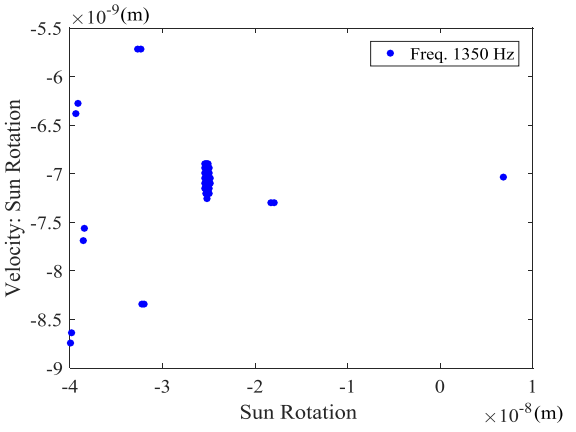

(b)

Fig. 8 Poincaré maps of the sun gear in: (a): 750 Hz and, (b): 1350 Hz.

4 SUMMARY AND CONCLUSIONS

In this study, linear and nonlinear dynamics of the single–stage spur planetary gear are developed and vibration behavior and natural frequencies of the system are analyzed. Linear and nonlinear systems are considered and equations of motion are solved numerically to study on the influence of the output flexibility on natural frequencies and vibration behavior of the system under nonlinear factors and fixed output. For first four natural frequencies, results of the linear system show that the most important effect of the output flexibility for the system is on the principal natural frequency. According to results of the nonlinear system under time– varying mesh stiffness, backlash of meshing gears and fixed output, vibration behaviors of components in translational directions are different because of chaotic phenomena.

REFERENCES

[1] Lin, J., Parker, R., Planetary Gear Parametric Instability Caused by Mesh Stiffness Variation, Journal of Sound and Vibration, Vol. 249, No. 1, 2002, pp. 129-145.

[2] Shi, J. F., Gou, X. F., and Zhu, L. Y., Modeling and Analysis of a Spur Gear Pair Considering Multi-State Mesh with Time-Varying Parameters and Backlash, Mechanism and Machine Theory, Vol. 134, 2019, pp. 582-603.

[3] Sun, T., Hu, H., Nonlinear Dynamics of a Planetary Gear System with Multiple Clearances, Mechanism and Machine Theory, Vol. 38, No. 12, 2003, pp. 1371-1390.

[4] Kahraman, A., Natural Modes of Planetary Gear Trains, Journal of Sound Vibration, Vol. 173, 1994, pp. 125-130.

[5] Kahraman, A., Load Sharing Characteristics of Planetary Transmissions, Mechanism and Machine Theory, Vol. 29, No. 8, 1994, pp. 1151-1165.

[6] Ambarisha, V. K., Parker, R. G., Suppression of Planet Mode Response in Planetary Gear Dynamics Through Mesh Phasing, Journal of Vibration and Acoustics, Vol. 128, No. 2, 2006, pp. 133-142.

[7] Lin, J., Parker, R. G., Analytical Characterization of the Unique Properties of Planetary Gear Free Vibration, Journal of Vibration and Acoustics, Vol. 121, No. 3, 1999, pp. 316-321.

[8] Parker, R. G., A Physical Explanation for the Effectiveness of Planet Phasing to Suppress Planetary Gear Vibration, Journal of Sound and Vibration, Vol. 236, No. 4, 2000, pp. 561-573.

[9] Lin, J., Parker, R. G., Natural Frequency Veering in Planetary Gears, Mechanics of Structures and Machines, Vol. 29, No. 4, 2001, pp. 411-429.

[10] Parker, R. G., Lin, J., Mesh Phasing Relationships in Planetary and Epicyclic Gears, J Mech Des, Vol. 126, No. 2, 2004, pp. 365-370.

[11] Tatar, A., Schwingshackl, C. W., and Friswell, M. I., Dynamic Behaviour of Three-Dimensional Planetary Geared Rotor Systems, Mechanism and Machine Theory, Vol. 134, 2019, pp. 39-56.

[12] Shahabi, A., Kazemian, A. H., Analysis of Time–Varying Mesh Stiffness for the Planetary Gear System with Analytical and Finite Element Methods, ADMT Journal, 2021.

[13] Shahabi, A., Kazemian, A. H., Dynamic and Vibration Analysis for Geometrical Structures of Planetary Gears, Journal of Solid Mechanics, Vol. 13, No. 4, 2021, pp. 384-398.

[14] Li, C. H., Chiou, H. S., Hung, C., Chang, Y, Y., and Yen, C. C., Integration of Finite Element Analysis and Optimum Design on Gear Systems, Finite Elements in Analysis and Design, Vol. 38, No. 3, 2002, pp. 179-192.

[15] Chen, Z. G., Shao, Y. M., and Lim, T. C., Non-Linear Dynamic Simulation of Gear Response Under the Idling Condition, International Journal of Automotive Technology, Vol. 13, No. 4, 2012, pp. 541-552.

[16] Masoumi, A., Pellicano, F., Samani, F. S., and Barbieri, M., Symmetry Breaking and Chaos-Induced Imbalance in Planetary Gears, Nonlinear Dynamics, Vol. 80, No. 1-2, 2015, pp. 561-582.

[17] Sainsot, P., Velex, P., and Duverger, O., Contribution of Gear Body to Tooth Deflections—A New Bidimensional Analytical Formula, J. Mech. Des., Vol. 126, No. 4, 2004, pp. 748-752.

[18] Kahraman, A., Free Torsional Vibration Characteristics of Compound Planetary Gear Sets, Mechanism and Machine Theory, Vol. 36, No. 8, 2001, pp. 953-971.

[19] Kiracofe, D. R., Parker, R. G., Structured Vibration Modes of General Compound Planetary Gear Systems, Journal of Vibration and Acoustics, Vol. 129, No. 1, 2006, pp. 1-16.

[20] Mabrouk, I, B., El Hami, A., Walha, L., Zghal, B., and Haddar, M., Dynamic Response Analysis of Vertical Axis Wind Turbine Geared Transmission System with Uncertainty, Engineering Structures, Vol. 139, 2017, pp. 170-179.

[21] Shahabi, A., Kazemian, A. H., Farahat, S., and Sarhaddi, F., The Influence of Engine Gyroscopic Moments on Vehicle Transient Handling, Proceedings of the Institution of Mechanical Engineers, Part D: Journal of Automobile Engineering, Vol. 235, No. 9, 2021, pp. 2425-2441.
[22] Shahabi, A., Kazemian, A. H., Farahat, S., and Sarhaddi, F., Dynamic Behavior of the Full-Car Model in the J-Turn Maneuver by Considering the Engine Gyroscopic Effects, Communications-Scientific letters of the University of Zilina, Vol. 23, No. 3, 2021, pp. B237-B249.
[23] Shahabi, A., Kazemian, A. H., Farahat, S., and Sarhaddi, F., Vehicle's Dynamic Behavior in Fishhook Maneuver by Considering the Engine Dynamics. ADMT Journal, Vol. 14, No. 2, 2021, 23-35.
[24] Shahabi, A., Kazemian, A. H., Farahat, S., and Sarhaddi, F, Wheel Slip Ratio Regulation for Investigating the Vehicle's Dynamic Behavior During Braking and Steering Input, Mechanics & Industry, Vol. 22, No. 17, 2021.
[25] Eritenel, T., Parker, R. G., Modal Properties of Three-Dimensional Helical Planetary Gears, Journal of Sound and Vibration, Vol. 325, No. 1-2, 2009, pp. 397-420.
[26] Bahk, C. J., Parker, R. G., Analytical Solution for the Nonlinear Dynamics of Planetary Gears, Journal of Computational and Nonlinear Dynamics, Vol. 6, No. 2, 2011.
[27] Orzechowski, G., Frączek, J., Integration of the Equations of Motion of Multibody Systems Using Absolute Nodal Coordinate Formulation, Acta Mechanica Et Automatic, Vol. 6, 2012, pp. 75-83.
[28] Wang, J., Rodriguez, J., and Keribar, R., Integration of Flexible Multibody Systems Using Radau IIA Algorithms, Journal of Computational and Nonlinear Dynamics, Vol. 5, No. 4, 2010.